Université Scientifique et Médicale de Grenoble

INSTITUT DES SCIENCES NUCLÉAIRES
DE GRENOBLE

53, avenue des Martyrs GRENOBLE

ISN 83.57. (RAPPORT INTERNE)
Octobre 1983

EXPERIMENTAL SET-UP FOR DIRECT MEASUREMENTS OF HEAVY ION REACTION CROSS SECTIONS

C. PERRIN, R. CHERKAOUI, A.J. COLE, A. GAMP, S. KOX,
N. LONGEQUEUE, J. MENET, J.B. VIANO

Laboratoire associé à l'Institut National de Physique Nucléaire et de Physique des Particules.

EXPERIMENTAL SET-UP FOR DIRECT MEASUREMENTS OF HEAVY ION REACTION CROSS SECTIONS.

C. PERRIN, R. CHERKAOUI, A.J. COLE, A. GAMP*, S.KOX, N. LONGEQUEUE, J. MENET and J.B. VIANO.

Institut des Sciences Nucléaires - 53, avenue des Martyrs 38026 - GRENOBLE Cedex

**also Hahn-Meitner Institut für Kernforschung, BERLIN*

ABSTRACT :

We describe an experimental set-up for measuring heavy-ion reaction cross sections with the transmission method. The experiment is operational in the energy range between 10 and 400 MeV/N.

I. Introduction

Total reaction cross section measurements with light projectiles have already been performed some 20 years ago [1-2] for comparison with optical model calculations. For these measurements the transmission method [3] which yields a direct, model independent value of the reaction cross section, was used.

In contrast to this, heavy ion reaction cross sections are usually obtained from elastic scattering by optical model [4-6] or phase shift analysis [7] or by use of the optical theorem [8-9] and are thus model dependent.

For incident energies $E_L < 10$ MeV/nucleon these methods are indeed quite convenient since here elastic scattering can be easily measured with good accuracy. At high incident energies this is no more the case because the major part of the elastic scattering is concentrated in a narrow cone around 0°. This facilitates on the other hand a direct measurement of the heavy ion reaction cross section.

Our measurements were motivated by experimental indications that the $^{12}C + ^{12}C$ reaction cross section does not saturate at the geometrical value as a function of incident energy but rather has an energy dependence similar to the free nucleon-nucleon total scattering cross section [10] . This was also suggested by microscopic calculations based on Glauber theory by DeVries and coworkers [11] .

In this article we present a heavy ion version of the transmission method which is operational in the energy range between 10 and 400 MeV/N.

In section II we describe the principle of the method and in section III its realization and its performance. Data handling and results are the subject of section IV. A summary and other possible applications of the set-up are given in section V.

II. Principle of the method.

The principle of the transmission method consists in counting the number of beam particles, N_B, incident on the target and the outgoing particles N_{el}, which have been scattered elastically or which have not interacted at all. The difference of these two numbers corresponds to the number of particles which have undergone a reaction. The reaction cross section is thus given by :

$$\sigma_R \sim \frac{1}{N_B} (N_B - N_{el})$$

It is not necessary to distinguish between the beam particles and elastically scattered particles in the vicinity of 0° since all these particles have the common feature of not having reacted.

It should be noted that N_B and N_{el} are statistically correlated. For an elastic scattering event, the same incoming beam particle gives rise to a count in the N_B counter and also, after the scattering process, in the N_{el} counter. Therefore the statistical error in σ_R is given by $\Delta\sigma_R \sim (N_B - N_{el})^{1/2}$. Here one assumes that the counting efficiency is 100 %. This can be checked by measurements without target (see sect.III e)

In principle the measurement of N_{el} requires a 4π counter geometry. In practice it is sufficient to measure up to a limiting angle θ_L beyond which elastic scattering can be treated as a small correction. This is generally the case for $\theta_L > 2$-3 times the grazing angle. The fact that we are counting the direct beam in this experiment necessitates beam intensities $N_B < 5 \cdot 10^4$ s^{-1}. This was achieved simply by closing appropriate pairs of

slits located close to the cyclotron beam extraction.
The reaction products resulting from slit scattering were eliminated by several succeding dipole magnets.

III. Realisation of the set-up and its performance.

a) General description.

A schematic view of our experiment is given in fig. 1. The beam particles were counted by the thin scintillator "1" and the active collimator "2". Behind the target the particles were identified and counted by a mosaic of 19 scintillators, the counters "3", "4" and "5", which was mounted in cylindrical symmetry on a "wheel" of $\emptyset$ = 44 cm.

The central detector "3" was centered on the beam axis and sourrounded by an inner ring of six counters "4" and by an outer ring of twelve counters "5". The scintillators were mounted on light guides of identical shape (see fig. 1). The latter were centered on XP 2020 Photomultipliers. For minimizing light losses the outer parts of the guides and scintillators were painted with white paint (NE 560).

Special care was taken that there were no inefficient regions between the central scintillator and the surrounding ones because the loss of only a small fraction of elastically scattered particles could give rise to a huge error in the determination of σ_R, as the following example will illustrate. With the above definitions of N_B and N_{el} one has $N_T \sigma_R = \frac{1}{N_B}(N_B - N_{el})$ where N_T denotes the number of target atoms per surface unit.

For a ^{12}C target of 5mg/cm² and a reaction cross section of 1 barn one has thus $\frac{1}{N_B}(N_B - N_{el}) = 2.5\ 10^{-4}$ or one reaction for 4000 incident particles. The consequence of losing or wrongly identifying one particle out of 4000 incident ones would be an error of the order of the effect to be measured. For this reason special care was taken to ensure geometrical

overlap of the scintillation material of the central detector and the surrounding ones. The outer scintillators (counter rings "4" and "5") were mechanically attached to the aluminium skeleton of the "wheel" by accurately machined metal supports which slightly overlapped the edges of the scintillation material (see fig.2). The inefficient region produced by these metal supports was thus known to high precision.

b) The counters in front of the target.

Counter "1" consisted of a thin scintillator coupled to a XP 2020 Photomultiplier. The purpose of this counter was twofold : it counted the number of incoming beam particles and it served as a start detector for the time-of-flight measurement (see below). Whenever the beam intensity became higher than $\sim 5 \cdot 10^4\ s^{-1}$ the experiment was blocked in order to avoid pile up.

The active collimator "2" was a thick scintillator with a hole centered on the beam axis. The whole system was aligned and the solid angles were defined such that beam particles passing through counter "1" and through the hole of counter "2" were detected in the central counter "3" behind the target.

Particles scattered off axis in the first scintillator were eliminated by an anticoincidence. A beam particle was thus defined as $N_B = 1.\bar{2}$ where the bar denotes the anticoincidence. The system was considered to be well aligned when all of the six counters "4" measured equal count rates and when the ratio of the counting rates of counters 2 and 1 did not exceed the factor 10^{-3}.

In order to be counted as a valid incident beam particle, the amplitude of a signal from a particle passing through the first scintillator had to fall into a well defined narrow band. Thus, sources of erroneous counting as triggering on noise or on residual beam impurities and pile up we eliminated.

Valid incident beam signals preceeded or followed by a signal from an adjacent beam burst($\Delta t \sim \pm 60$ ns) were also rejected.

c) The counters behind the target.

In the light particle versions of this experiment [1,2] a thick stop detector (scintillator), which measured directly the energy of the particles could be used. In heavy ion collisions, however, a large variety of quasi elastic reaction products occurs which all have a velocity similar to that of the elastically scattered particles. In a thick scintillator all these particles would cause similar light output and distinction between quasi elastic reaction products and elastic scattering would be very critical or impossible. Finally, stopping of heavy ions in the scintillation material may result in important radiation damage.

In order to avoid all these problems, we chose the thickness of the scintillators behind the target such that, for a given energy, the elastically scattered particles were stopped only in the light guide behind the scintillators. Thus, the light signals ΔL issuing from these detectors correspond to the differential energy loss ΔE (see below).

The time-of-flight and the ΔL signals of particles arriving in the detector behind the target were registered respectively in time-to-digital converters and ADCs. The linear dynode photomultiplier outputs were directly connected to the entries of the charge integrating ADCs. Events corresponding to the direct beam were not written on magnetic tape but rather counted by a scaler. The rejection of these events was achieved by means of a fast anticoincidence unit [12] which enabled us to define a very narrow time window (< 2 ns) centered around the time-of-flight of a beam particle arriving in the central detector.

The charge resolution is demonstrated in figs. 3 and 4. In fig. 3 the ΔL, t plot of the outgoing fragments resulting from $^{12}C + ^{12}C$ collisions at 30 MeV/N is shown for one of the counters "4". In fig. 4 the projection of

A similar plot on the ΔL axis is shown for ^{20}Ne + ^{12}C collisions at 30 MeV/N. Here all the projected particles have essentially the same velocity E/A. Since $\Delta E \sim \frac{A}{E} Z^2 \sim Z^2$ one expects also that the separation ΔL of adjacent charges increases with element number. The measured relation between ΔL and element number is displayed in fig. 5 and compared with semiempirical expressions from ref. 13.

As one can infer from figs. 3 and 4, the charge identification of our counters is sufficiently good for separating the beam charge (^{12}C or ^{20}Ne) from adjacent ones. Isotope separation is, however, not possible and corrections to the data for neutron transfer have to be taken into account.

As stated above the cone spanned by the detector behind the target has to be sufficiently large so that the elastic scattering ocurring at angles larger than the cone opening can be treated as a small correction. This is generally the case for cone openings twice or three times as big as the grazing angle. On the other hand, taking into account our time resolution of typically 500 ps, the time of flight measurement necessitates a minimum distance between the target and the last detector. All this results in the counter dimensions and distances listed in table 1.

d) Targets.

In this experiment the accurate determination of the target thickness ΔT is of crucial importance since the error in this quantity contributes fully to the absolute error in our measured reaction cross-section. Therefore two independent methods of measuring ΔT, namely weighing and α-energy loss measurements were employed and found to give consistent results.

It was also checked that the angular straggling due to the relatively thick targets (see table 1) did not exceed the angular cone defined by the central detector.

c) Reliability tests.

We tested the reliability of our experimental set-up by target in-target out measurements. In the ideal case no reactions at all should be observed for the target out case, i.e. $N_B = N_{el}$. In reality there are already reactions in the first scintillator and also in the detector behind the target. The ratio between the number of reactions with and without target was typically $R(^{\text{target in}}/_{\text{target out}}) \approx 30$ for a ^{12}C target of 30 mg/cm^2.

This result also guarantees that the detection efficiency of each of the detectors is sufficiently close to 100 %. As is easily shown we are loosing less than one particle out of $2 \cdot 10^4$ incident ones due to detection inefficiencies (cf. the example given in sect.IIIa).

Since in this experiment we are counting the direct beam, the beam intensity was limited to some $4 \cdot 10^4$ s^{-1}. With this intensity the completition of a given measurement could be achieved within a few hours. It should also be noted that, in order to avoid errors due to pile up, the entire electronics was set-up on the nanosecond level.

IV. Data handling and results.

So far we have measured the reaction cross section for $^{12}C + ^{12}C$ collisions at 9.3, 30 and 83 MeV/N [14] and also for a variety of heavier target-projectile combinations at 30 and 83 MeV/N [15]. The experiments at 9.3 and 30 MeV/N were performed at the Grenoble cyclotron facility SARA, the 83 MeV/N ^{12}C beam was delivered by the CERN synchrocyclotron.

The light output and time of flight information from each of the detectors "3", "4" and "5" were stored on magnetic tape. For the central detector (i.e. detector "3" which sees the direct beam), a narrow time window including the beam and elastically scattered particles was excluded from the recorded information in order to limit the counting rate at the computer.

Even without using the recorded information one can define a raw or uncorrected reaction cross section $\sigma_R(\text{raw})$ simply by counting events of the type $N_B.\bar{3}$. That means that, for the moment all the events of the central counter "3" are considered to be elastic. We define :

$$\sigma_R(\text{raw}) = \frac{1}{N_B N_T}\left[N_B.\bar{3}(\text{target in}) - N_B.\bar{3}(\text{target out})\right]$$

The necessity of the target in - target out measurements has already been pointed out. In addition, they permit to monitor the stability of the result against small, ever present variations in the beam intensity. We found that $\sigma_R(\text{raw})$ was stable to within 2 %.

The final value of σ_R is related to the raw value by the equation

$$\sigma_R = \sigma'_R(\text{raw}) - \sigma_{elast}(\theta>\theta_3)$$

where $\sigma'_R(\text{raw})$ is obtained from $\sigma_R(\text{raw})$ subtracting a correction due to reaction products falling into counter "3". The major part of $\sigma_{elast}(\theta>\theta_3)$ is measured by the counter rings "4" and "5". Our time and ΔL resolution was, however, not sufficiently good for unambiguous separation of elastic from inelastic scattering and from neutron transfer reactions. Thus, these measured quantities are subject to some corrections which are described in detail in ref.14. It should be emphasized, however, that the sum of these corrections does not exceed 10 % of the reaction cross section.

An example of our experimental results is shown in fig.6. The errors contain a contribution of about 1% due to counting statistics and some 2% due to the error in target thickness measurement. The remaining error comes from the uncertainties in estimating the corrections (see ref.14).

Recently we have also performed reaction cross section measurements with ^{20}Ne projectiles. Heavier projectiles have not yet been investigated. A test run with Ar projectiles is planned in order to see whether the ΔL resolution will still be sufficient to separate adjacent charges in this region. Here th

fact that at energies > 30 MeV/N the outgoing quasielastic reaction products all have essentially beam velocity may be helpful (see fig. 4).

V. Summary and other applications of the set-up.

We have described an experimental set-up for measuring heavy ion reaction cross section with the transmission method.

The originality of our experiment lies in the fact that we are identifying the elastically scattered heavy ions by a ΔLight-time-of-flight measurement (see sect.III c). Even though our method is direct and model independent some corrections have to be applied to the measurement of N_{el} because the time-of-flight resolution is not sufficient for unambigious separation of the excitation of low lying inelastic levels from pure elastic scattering. Furthermore, although the ΔL measurement allows the separation of the projectile charge from adjacent ones, at least up to ^{20}Ne projectiles, neutron transfer has to be corrected for (see sect. IV).

The sum of these corrections never exceeded 10 % of the reaction cross section.

With this set-up heavy ion reaction cross sections have been measured with a precision of the order of 5 %.

The use of a high resolution counter like an ionisation chamber [16] instead of our scintillators could yield a better identification of elastic scattering. On the other hand such a counter would be at least ten times slower than the present one which is still operational at beam intensities of $4 \cdot 10^4\ s^{-1}$. Furthermore, the number of reactions in our scintillators is limited since we stop the particles only in the light guides behind. Thus, background or zero effects are limited to a reasonable amount ($\approx \frac{1}{30}$, see sect. III c).

Since our counter arrangement consists of 19 independent counters one may also use it as a multiplicity counter in heavy-ion-light particle coincidence experiments. The large dynamic range (see figs.3, 4) of each of the counters permits also the simultaneous measurement of correlations between heavier fragments. Such experiments are presently being performed.

Acknowledgements.

We would like to express our gratitude to L. Pitrot, J.P. Cremet and P. Oustric for technical support in the early stage of the experiment. One us (A.G.) acknowledges the hospitality received from the I.S.N. during his stay in Grenoble.

TABLE CAPTION

TABLE 1 : Distances between the various counters and the resulting opening angles of the detectors behind the target. The three values given correspond to the three energies of 9.3, 30 and 83 MeV/N respectively. The grazing angles for $^{12}C + ^{12}C$ collisions are also indicated.

Table 1

Distances [cm]				Scintillators			Angles [Deg]		Diameter of active collimator "2" [cm]
	"2"	Target	"3"	Counter	Thickness [mm]	Type			
	13	36	154		0.03	NE 102		2.14	5
"1"	52	75	293	"1"	0.125	ref 17	Θ_3 :	1.19	3
	52	75	493		0.2	ref 17		0.604	3
		23	141		0.4	NE 102		5.79	
"2"		23	241	"2"	1.0	NE 102	Θ_4 :	3.19	
		23	441		1.0	NE 102		1.64	4.23
			118		0.2	ref 17		10.55	Grazing angle (lab) 1.2
Target			218	"3","4","5"	1.0	ref 17	Θ_5 :	5.79	[Deg] 0.44
			418		5.0	NE 110		3.01	

FIGURE CAPTIONS

FIG. 1 : Experimental set-up

The number of beam particles N_B incident on the target is defined by $N_B = 1.\bar{2}$ where the bar denotes an anticoincidence. The number of particles N_{el} which have not given rise to a reaction is determined by the counters "3","4"and"5"(19 Photomultipliers in total). The reaction cross section is given by $\sigma_R \sim \frac{1}{N_B}(N_B - N_{el})$. The distances between the counters and the values of the relevant angles are listed in table 1.

FIG. 2 : Schematic view of the counter arrangement behind the target. The dashed areas represent the supports of the counters "4" and "5". These supports were designed such that the radial symmetry of the counters around the beam axis was conserved. Thus the correction to be applied to the number of particles detected in the active part of the counter was a simple multiplicative factor which varied from 1.1 to 1.2.

FIG. 3 : Example of charge separation in the $\Delta L - t$ plane for $^{12}C + ^{12}C$ collisions at $E_{lab} = 30$ MeV/N.

FIG. 4 : Projected charge spectrum of $^{20}Ne + ^{12}C$ collisions at $E_{lab} = 30$ MeV/ All the projected events have about the same (beam) velocity. Therefore the separation of adjacent charges increases with element numbe

FIG. 5 : Measured photomultiplier pulse height as a function of element number. All the heavy ions have approximately the same velocity $\frac{E}{A}$. The light output is well described by the semiempirical relations (full curve) from ref. 13. For comparison we also show $\Delta L \sim Z^2$ (broken curve).

FIG. 6 : Total reaction cross section for $^{12}C + ^{12}C$ collisions as a function of incident energy. The three values measured with our direct method are indicated by the full triangles. The agreement with other data is apparent. The full points were obtained by a parametrized phase shift analysis [7] of the data from ref. 18, the other data points (only typical error bars are given) labeled o, X, + and Δ are taken from refs. 7, 6, 4 and 10 respectively.

REFERENCES

(1) B.D. Wilkins and G. Igo, Phys. Rev. 129, 2198 (1963).

(2) A. Budzanowski, K. Grotowski, J. Kuzminski, H. Niewodniczanski, A. Stralkowski, S. Sykutowski, J. Szmider and R. Wolski, Nuclear. Phys. A106, 21 (1968).

(3) T.J. Gooding, Nucl. Phys. 12, 241 (1959).

(4) M. Buenerd, P. Martin, R. Bertholet, C. Guet, M. Maurel, J. Mougey H. Nifenecker, J. Pinston, P. Perrin, F. Schussler, J. Julien, J.P. Bondorf, L. Carlen, H.A. Gustafsson, B. Jakobsson, T. Johansson, P. Kristiansson, O.B. Nielsen, A. Oskarsson, I. Otterlund, H. Ryde, D. Schröder, and G. Tibell, Phys. Rev. C26, 1299 (1982).
M. Buenerd, in Proceedings of the XXth Winter Meeting on Nuclear Physics, Bormio, Italy, 1982.

(5) M.E. Brandan and A. Menchaca-Rocha, Phys. Rev. C23, 1272 (1981).

(6) H.G. Bohlen, M.R. Clover, G. Ingold, H. Lettau, W.v. Oertzen, Z. Phys. A308, 121 (1982).

(7) A.J. Cole, W.D.M. Rae, M.E. Brandan, A. Dacal, B.G. Harvey, R. Legrain, M.J. Murphy, and R.G. Stokstad, Phys. Rev. Lett. 47, 1705 (1981).

(8) H. Oeschler, H.L. Harney, D.L. Millis, K.S. Sim, Nucl. Phys. A325, 463 (1979).

(9) C. Marty, Z. Phys. A309, 261 (1983).

(10) J. Jaros, A. Wagner, L. Anderson, O. Chamberlain, R.Z. Fuzesy, J. Gallup, W. Gorn, L. Schroeder, S. Shannon, G. Shapiro and H. Steiner Phys. Rev. C18, 2273 (1978)

(11) R.M. DeVries and J.C. Peng, Phys. Rev. Lett. 43, 1373 (1979)
R.M. DeVries and J.C. Peng, Phys. Rev. C22, 1055 (1980).

(12) J.P. Cromet, ISN Grenoble, Annual report, 21, (1980)
The principle of this coincidence unit is based on the addition of two fast NIM signals. The coincidence width is defined by the variable amplitude level of a fast comparator.

(13) F.D. Bechetti, C.E. Thorn and M.J. Levine, Nuclear Instruments and methods, 138, 93 (1976).
M. Buenerd, D.L. Hendrie, U. Jahnke, J. Mahoney, A. Menchaca-Rocha, C. Olmer and D.K. Scott, Nuclear Instruments and Methods, 136, 173 (1976).

(14) C. Perrin, S. Kox, N. Longequeue, J.B. Viano, M. Buenerd, R. Cherkaoui, A.J. Cole, A. Gamp, J. Menet, R. Ost, R. Berthelet, C. Guet, J. Pinston Phys. Rev. Lett. 49, 1905 (1982).

(15) A. Gamp, in Proceedings of the XXI Winter Meeting on Nuclear Physics, Bormio, Italy, 1983.

(16) A. Gamp and H.L. Harney, Orsay Preprint IPNO - Phn 78-20.

(17) These scintillators were manufactured by C.E.N. Saclay, S.T.I.P.E.

(18) R.G. Stokstad, R.M. Wieland, G.R. Satchler, C.B. Fulmer, D.C. Hensley, S. Raman, L.D. Rickertsen, A.H. Snell, and P.H. Stelson, Phys. Rev. C20, 655 (1979).

FIGURE 1

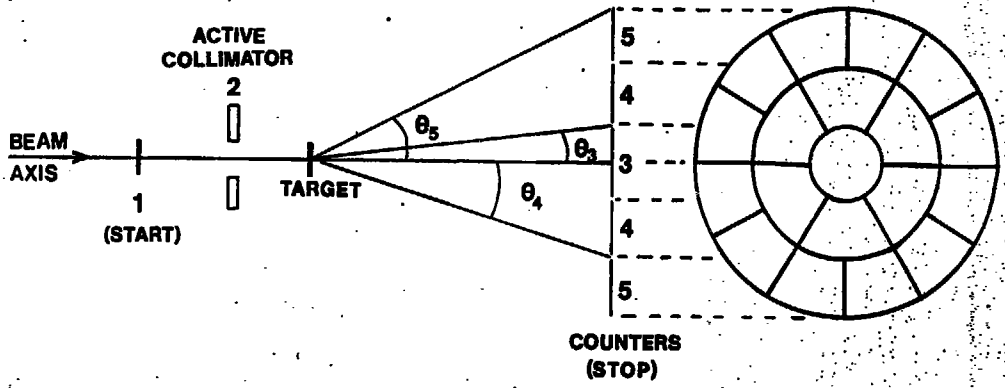
ACTIVE
COLLIMATOR
2
BEAM
AXIS
1
(START)
TARGET
θ5
θ3
θ4
5
4
3
4
5
COUNTERS
(STOP)

Fig 2

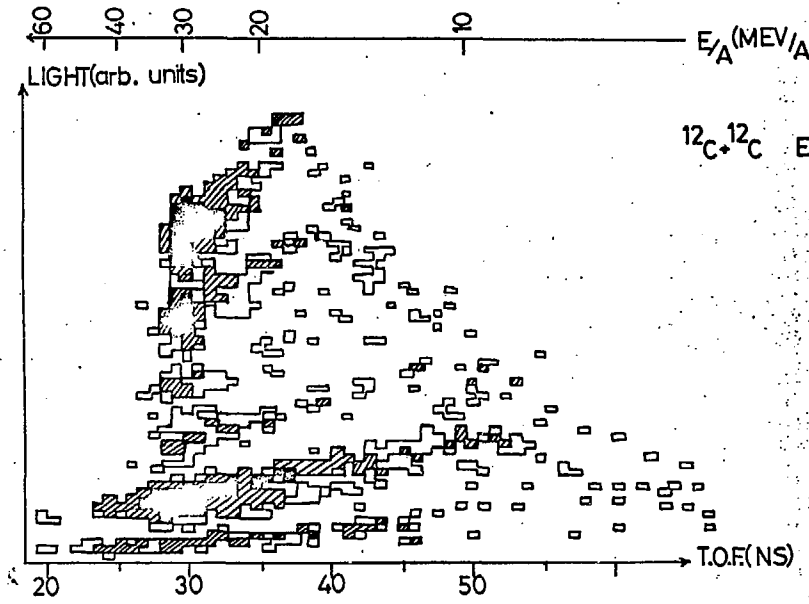
60
40
30
20
10
E/A(MEV/A)
LIGHT(arb. units)
12C+12C Elab=30 MEV/A
θ=2.2°
20
30
40
50
T.O.F.(NS)

Fig.3

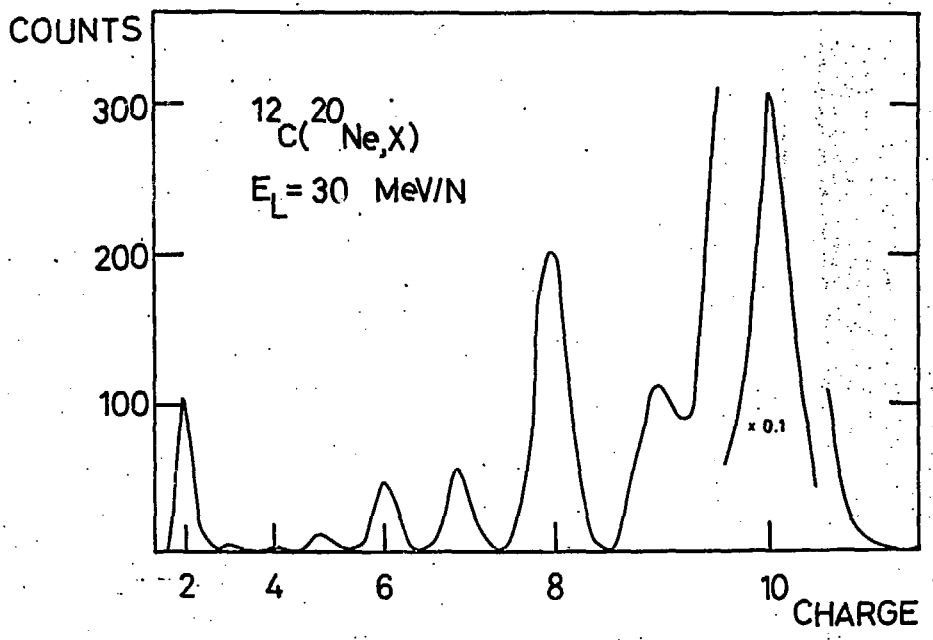

Fig. 4

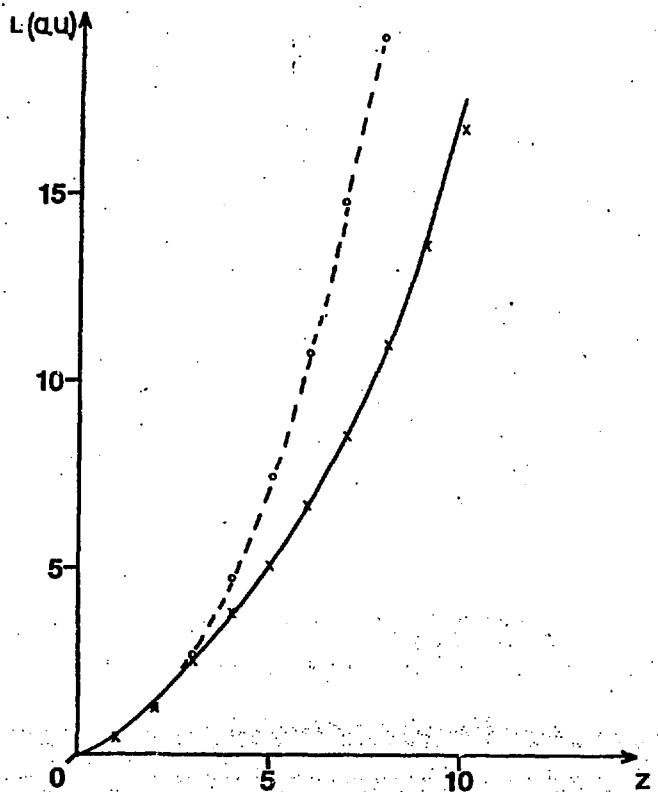

Fig. 5

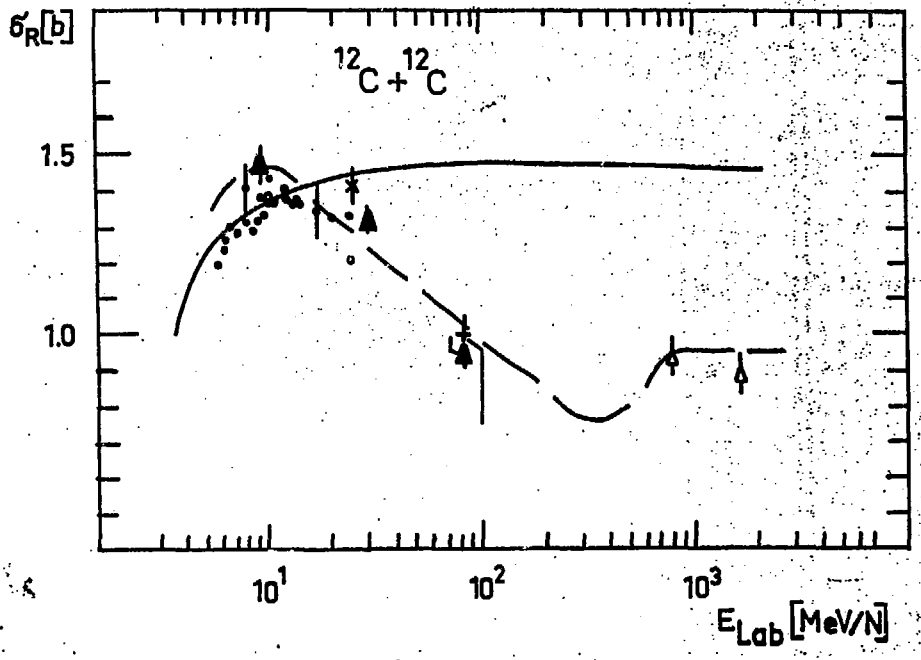

Fig. 6